

# GLAO IN THE VISIBLE: THE SAM EXPERIENCE

Andrei Tokovinin<sup>a</sup>

Cerro Tololo Interamerican Observatory, Casilla 603, La Serena, Chile

**Abstract.** The SOAR adaptive module (SAM) is going through science verification and is offered in shared risk in 2013B. It is a GLAO instrument with a UV Rayleigh laser to improve image quality in the visible. The resolution in closed loop reaches  $0.25''$  in the  $I$  band (typical  $0.4''$  in  $I$ ,  $0.5''$  in  $V$ ). Substantial gain over open-loop resolution was reached on 6 nights out of 11 in 2012-2013, under calm free-atmosphere conditions. The compensation is uniform over the 3-arcmin. field. We discuss operational aspects of SAM and its potential science programs. Critical evaluation of the design might be of interest to other AO instruments. We stress the need to provide GLAO correction at visible wavelengths for ELTs and the relevance of SAM from this perspective.

## 1 Introduction: instrument and its commissioning

The SOAR Adaptive Module, SAM, is a ground-layer adaptive optics (GLAO) instrument using a Rayleigh laser guide star (LGS) [4–7]. The project was started in 2001, 12 years ago, with the aim to improve seeing at optical wavelengths. The idea of GLAO was fresh at that time. Even now, when various GLAO instruments are being designed and constructed, its application in the visible remains unpopular. SAM is a unique facility instrument implementing this idea.

Figure 1 is a simplified diagram of the SAM AO module illustrating its differences from “standard” AO systems. First, the tip and tilt (tt) compensation is provided by the actuated tertiary mirror of the 4.1-m SOAR telescope, upstream from the instrument. Second, tt is sensed by two small guide probes deployed in the input (un-corrected) focal plane. This avoids the need to split photons in wavelength between science and guide channels. The probes sample the  $5'$  square patrol field outside the  $3'$  science field. In this design the tilts introduced by the deformable mirror (DM) are not sensed, but the DM control is tilt-free. The third SAM particularity is the use of a UV Rayleigh LGS at 7 km from the telescope. Its light is focused well behind the nominal telescope focal plane, the light path of LGS photons inside SAM is very different from the the starlight. Nevertheless, major non-common-path errors were avoided.

SAM can feed corrected images to its internal CCD detector, SAMI (4K×4K CCD) or to a visitor instrument (this port is now occupied by the speckle camera). The beam at the visitor port has the same scale,  $f$ -ratio, distance, and pupil position as in the main telescope.

SAM received first laser light in March 2011. Good correction was achieved a year later. Figure 2 resumes SAM experience during 11 nights of engineering and commissioning between March 2012 and March 2013. On six nights, reasonably good seeing improvement was achieved. The shutdown periods were used to improve the thermal environment of the laser launch telescope (LLT) to get smaller LGS spots and for other technical work and repairs. Some data obtained in 2012 turned out to be scientifically useful, resulting in the first science publication [2]. The science verification began in February 2013; it will be continued in the 2013B semester along with engineering and first shared-risk programs.

---

<sup>a</sup> atokovinin@ctio.noao.edu

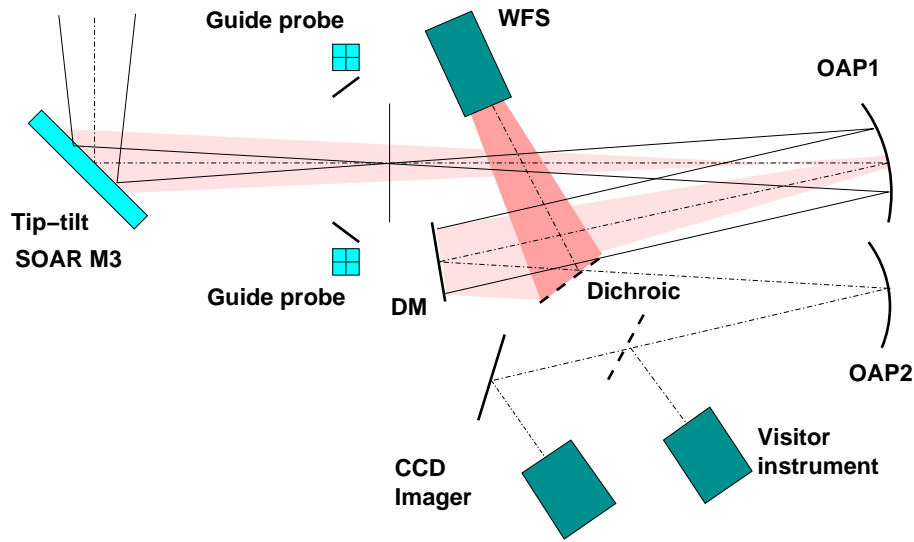


Fig. 1. Schematic light path through SAM.

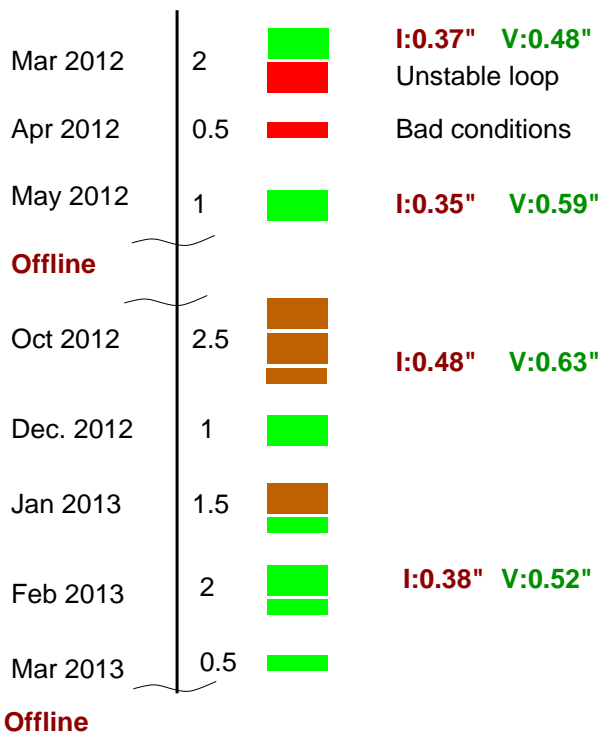


Fig. 2. Summary of SAM commissioning over the last year. The approximate number of nights used by each run is indicated. The nights are coded by the green color when a useful performance was achieved, by brown when SAM gave little gain in resolution, by red when the instrument was not operational. Median FWHM image quality in the *I* and *V* bands is indicated for some nights. Periods when the instrument was offline (shutdowns) are marked.

## 2 Operation and delivered image quality

The restrictions on laser propagation imposed by the laser clearing house (LCH) require submission of target lists few days in advance. The nominal SAM avoidance cone of  $0.2^\circ$  is small enough to allow science observations (the duration of authorized propagation windows varies from few minutes to more than an hour). The laser is shuttered automatically when the propagation is forbidden.

The acquisition of LGS and closure of the laser loop turned out to be easy and routine operations. Typical time between the end of observations of one target and beginning of the next target is about 15 min (record 10 min). Most of this time is spent for acquisition of two guide stars. As the field of the probes is small,  $3''$ , pre-imaging with SAMI and identification of

a star with known position in the image are required to establish the exact telescope pointing. So far, we were able to find guide stars brighter than  $R = 18$  in all fields, confirming the nearly complete sky coverage of SAM.

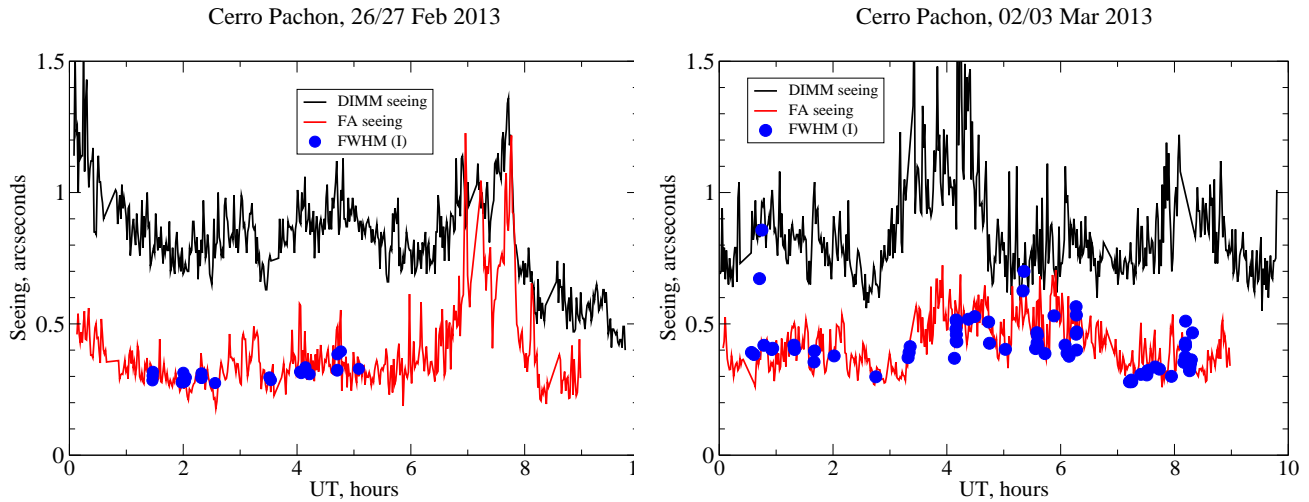


**Fig. 3.** Atmospheric conditions on the two SAM nights. The black lines show the total (DIMM) seeing, the red lines the free-atmosphere seeing (MASS, above 0.5 km) at zenith. The blue dots are average FWHM of closed-loop images in SAMI ( $I$  filter, no correction to zenith).

Figure 11 in [7] gives cumulative histograms of FWHM resolution in closed and opened loop for the night of March 6, 2012. Similar performance was reached on other “good” nights. Figure 3 shows the evolution of total and free-atmosphere seeing measured by the MASS-DIMM site monitor at Cerro Pachón on two nights. The average FWHM resolution in the SAMI images in closed loop in the  $I$  band (hereafter delivered image quality, DIQ) is over-plotted; it is in remarkably good agreement with the free-atmosphere seeing. The best DIQ in  $I$  is  $0.28''$ . The best DIQ in the  $B$  filter reached on Feb. 26, 2013, was from  $0.36''$  to  $0.45''$ .

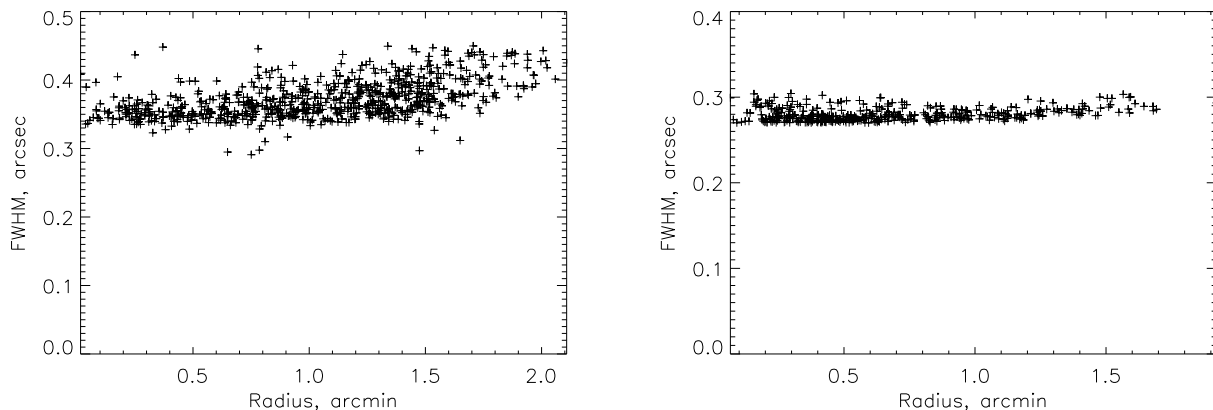


**Fig. 4.** FWHM uniformity over the field. March 2/3, 2013,  $I$  band. Left: UT 4:08,  $0.369''$ ; right: UT 7:13,  $0.280''$  (see Fig. 3, right).

The correction over the full 3' field is normally quite uniform, with DIQ variation of few percent. The DIQ variation is larger in the  $I$  band, where the correction is best. Figure 4 gives quantitative assessment of the DIQ uniformity for two images taken on March 2, 2013. For the first image at UT 4:08, there was some turbulence in the “gray zone” at  $\sim 0.5$  km that degraded the on-axis DIQ and caused further degradation off-axis. Few hours later the conditions improved (see Fig. 3, right), and the DIQ uniformity over the field became excellent.

On May 8, 2012, the DIQ was not uniform, showing a gradient over the field [7]. Most likely, this was caused by the fast wind speed near the ground combined with the time-lag effect of the AO loop. Despite the DIQ non-uniformity, good-quality photometry of dense stellar field is reported in [2]. The loop frequency was doubled to 440 Hz since January 2013, when we changed the WFS detector readout mode to 2x2 binning.

The point spread function (PSF) in closed loop is different from the atmospheric PSF: it has a sharper core and a stronger halo. Such PSF can be approximated by a Moffat function with index  $\beta$  from 1.5 to 2 [7]. The residual phase structure function after correction in SAM depends on the distance almost linearly [5], producing a peaked PSF with  $\beta = 1.5$ .

The closed-loop PSF is usually very symmetric, with ellipticity of  $< 5\%$ . However, under 2x2 binning mode one “dead” row of pixels in the WFS CCD created substantial systematic offsets in the spot centroids. This, in turn, produced a warp in the wavefront and faint “tails” in the PSF. This defect is corrected by introducing suitable offsets to compensate for the missing signal.

### 3 Science with SAM

Tremendous scientific impact of high-resolution optical images from the Hubble Space Telescope (HST) shows importance of the optical spectral region to study major atomic transitions, stellar spectra, etc. So far, ground-based AO systems provide correction only in the near-IR. SAM is the first step towards competing with the HST in the visible. Its DIQ is still a factor of 4 worse, however, so we have to look for new applications where the larger telescope diameter, 3' field, or mere availability of SAM can balance the resolution advantage of the HST. The science verification (SV) proposals for SAM give the first glimpse of its potential niches. We received 16 SV proposals and classify them broadly into several areas.

**Stellar clusters** are the first and most obvious application of SAM. Its gain in the DIQ translates to the deeper magnitude limit, especially in the crowded fields [3]. Large corrected field of SAM is essential; synergy with GEMS is possible. SAM can address various aspects of globular clusters [2] and clusters in the Magellanic clouds. Resolved stellar populations in nearby galaxies belong to the same category. One SV program aims at photometric monitoring of bright stars in the globular cluster M5.

**Nebulae** are targets where the SAM field and wavelength range matter. Figure 5 shows an exquisite image of the planetary nebular NGC 2440 obtained with SAM in February 2013. One SV proposal aims at observing planetary nebulae with a large dynamic range to characterize weak surrounding emissions. Nebulae associated with star formation (e.g. Herbig-Haro objects, proplyds) is another interesting class of targets for SAM. On the other hand, SAM is not useful for observations of very faint nebulae with low surface brightness because their detection against sky background requires signal binning, with associated loss of the resolution.

**Small targets**, on the contrary, do not use the full SAM corrected field and require imaging of the on-axis object with the highest possible resolution. SAM offers here its full sky coverage

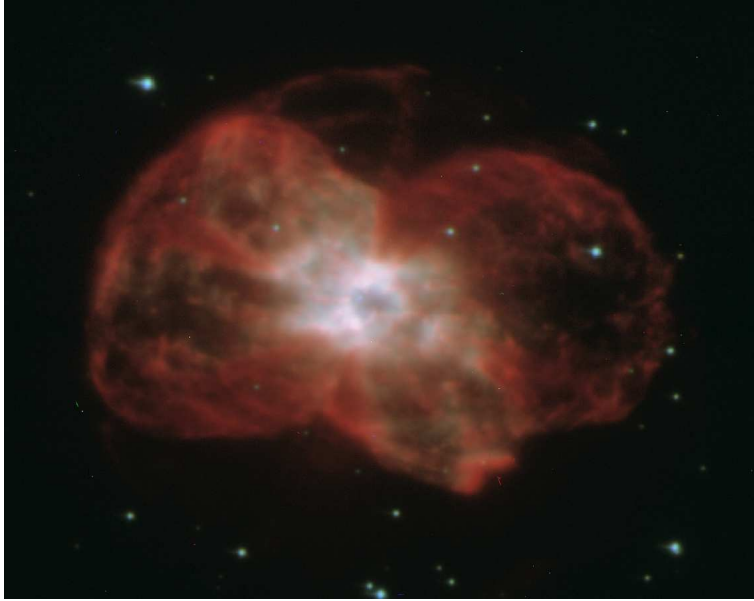


**Fig. 5.** Composite color image of planetary nebula NGC 2440 (fragment). The R,G,B colors correspond to the  $H\alpha$ ,  $V$ ,  $B$  filters, with 60-s exposures in each filter and the FWHM resolution of  $0.36''$  in  $B$  and  $0.28''$  in  $I$ .

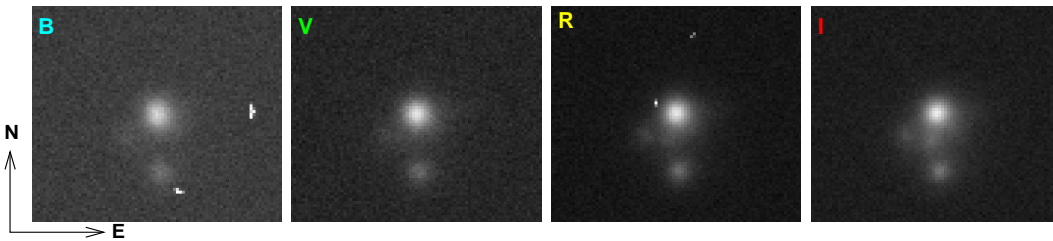


**Fig. 6.** Images of lensed quasar SDSS\_0924 in the  $BVRI$  bands with 5-min. exposure in closed loop taken on Jan. 29/30, 2013. Each fragment is  $6.7''$  across, the distance between N and S components is  $1.9''$ , the DIQ varies from  $0.5''$  in  $B$  to  $0.4''$  in  $I$ .

and high sensitivity. The SV programs address a range of such targets: distant galaxies, gravitational arcs, lensed quasars (Fig. 6), and even solar-system objects like asteroids or Pluto. This class also includes binary and multiple stars. Although binaries are better studied by classical near-IR AO systems such as NACO (diffraction-limited resolution at 8-m telescopes), the availability of SAM can make this application attractive. SAM potential in this area can be further enhanced in the future by adding a small-field IR camera.

**Spectroscopy.** In the future, SAM can compete with the HST in integral-field spectroscopy. The size of the resolution element is often dictated by the photon flux rather than by the DIQ. Larger aperture of SOAR+SAM will reach fainter targets compared to the HST; this advantage will also be exploited at the VLT by MUSE [1]. It is planned that the fiber-based integral-field unit (IFU), SIFS, will work with SAM after being commissioned in the seeing-limited mode. A similar or better performance could possibly be reached by building an IFU fiber feed for the Goodman spectrograph, which is located side-by-side with SAM. Construction of a multi-slit spectrometer for SAM is being explored as well.

## 4 Lessons learned

Development of the laser-assisted AO facility instrument at CTIO was a tough challenge, considering the lack of prior experience in AO in our organization. The project took longer than expected, with corresponding increase in the manpower cost. Most of the delay was caused by the design, fabrication, and integration of general (not AO-specific) opto-mechanics and software. The risk management strategy (early prototyping of critical components and subsystems) was successful in avoiding major setbacks and reworks.

The choice of the industrial laser (Q-302HD from JDSU, tripled Nd:YAG) proved to be correct. So far it works without faults and gives on average 7.5 W power with good beam quality. The design of the SAM laser system in general – beam transfer, laser launch telescope (LLT), beam control and safety – is validated by the practice. For example, a burned insect in the beam transfer optics was detected remotely by unusual signals in the photo-diodes sampling the outgoing beam. The goal of having “set and forget” LGS is almost met. Over-specifying the laser power has been a wise decision, too. We had trouble with the thermal behavior of the LLT main mirror (its attachment was modified as a result) and with the laser spot degradation by the warm air produced by the LLT electronics (now fixed by switching on motor controllers only during LGS acquisition).

SAM does not produce scientific data by itself, it is just an intermediate stage between the telescope and the science instrument. Ideally, SAM operation should be as simple and transparent as possible. In reality the complexity of the system (number of parameters and components) translates into operational complexity. During 2.5 years of SAM commissioning (first with natural guide star, then with laser) a significant progress has been achieved. The instrument is controlled by a single top-level software, many routine operations and checks are automated by scripts, the observing procedure has been developed and tested. The operation of the AO system, even simplified, still requires a trained person, the *SAM operator*. In the future it might become feasible to transfer SAM operation to the telescope operators. Still, preparation of the instrument for the observing runs is and will be done by trained engineers and/or scientists.

The large number of controlled motions and components presents a major risk for reliability and maintenance of SAM. During short lifetime of the instrument, several critical components were already repaired (the SDSU-III controller of the WFS CCD, high voltage DM driver, piezoelectric platform and its driver in the LLT, motion controllers and actuators). Substantial fraction of downtime was caused by the software, mainly due to communication problems between the software components or with the hardware.

The reality of SAM operation differs from its original error budget [5], as in every real AO instrument. The typical FWHM of the LGS spots is 1.6", larger than 1" assumed originally (although sometimes we do get 1" spots). The return flux, although amply sufficient, is less than predicted; it depends on the seeing conditions and on the angle of the instrument rotator (due to imperfect polarization adjustment in the WFS). As a result, the rms centroid errors are typically between 0.1 and 0.2 pixels (0.07" to 0.14"). The combination of the WFS geometry (rectangular 10×10, 72 working sub-apertures) and DM geometry (radial with 60 electrodes) allows us to correct about 40 system modes. Under typical ground-layer seeing between 0.6" and 1" the correction in the visible is only partial, explaining why the DIQ is worse at shorter wavelengths. If SAM were designed today, we would opt for a higher correction order to boost its performance in the blue region of the spectrum. Availability of EM CCDs with low noise makes this possible without increasing the laser power.

## 5 Relevance to ELTs

Despite strong appeal of diffraction-limited turbulence correction, the “ $D^4$  gain”, all ELTs will operate in the seeing-limited mode at optical wavelengths during some non-negligible fraction of their time. The field of view will be sufficiently small to allow substantial resolution gain from partial compensation of the ground-layer turbulence, as demonstrated by SAM. This gain will boost the ELT performance in virtually all observing modes, from background-limited spectroscopy of very faint sources to high-resolution spectroscopy of nearby stars.

The science case for implementing visible-light GLAO at ELTs is strong. Availability of correctors (deformable secondaries) in the ELT optics takes this goal one step closer to reality. We only need to provide a control signal to drive those DMs. For visible-light correction, a relatively high order is needed, hence the use of LGS is imperative (NGS-based GLAO systems have a chance to work only in the IR and with a limited sky coverage). For the same reason, multiple sodium beacons implemented for laser tomography will not be as good as Rayleigh LGS. However, a straightforward scaling of SAM will not work either, more complex solutions will be needed.

One lesson of SAM is worth noting. The resolution of the image in Fig. 5 taken around UT 2:10 on February 26/27, 2013, is  $0.36''$  even in the  $B$  band where the SAM compensation order is too low for providing a substantial gain. Yet the seeing reported by DIMM (Fig. 3, left) was about  $0.75''$ , slightly worse than median. The only reasonable explanation is that DIMM was strongly affected by the local turbulence and that the total seeing experienced at this moment at SOAR was much better. SAM did little to correct it. And yet there was a good reason to use SAM because it corrected residual low-order optical aberrations of the telescope and large-scale components of the dome seeing (optical testing at large telescopes shows that low-order aberrations always fluctuate, being affected by the air stratification in the dome).

The enclosures of ELTs will be much larger than the SOAR dome. It is naive to assume that ELTs will be free of thermal air disturbances and that optical aberrations and vibration will be actively corrected in real time, accessing the pristine free-air seeing at the height of the ELT dome. Even in the absence of ground-layer turbulence (as likely happened at SOAR on Feb. 26), a GLAO system at ELTs has a lot of things to correct and will deliver a worthy gain in performance.

## References

1. Bacon, R., Accardo, M., Adjali, L. et al. Proc. SPIE, **7735** (2012), 7
2. Fraga, L., Kunder, A., Tokovinin, A. AJ, **145**, (2013) 165
3. Olsen, K. A. G., Blum, R. D., & Rigaut, F. AJ, **126**, (2003), 452
4. Tokovinin, A., Gregory, B., Schwarz, H.E. et al. Proc. SPIE, **4839**, (2002) 673.
5. Tokovinin, A. Proc. SPIE, **7015**, (2008) 77
6. Tokovinin A., Tighe R., Schurter P. et al. Proc. SPIE, **7736**, (2010) 132
7. Tokovinin, A., Tighe, R., Schurter, P. et al. Proc. SPIE, **8447**, (2012) 166